

Geophysical Research Letters

RESEARCH LETTER

10.1029/2020GL089005

Key Points:

- Radio frequency lightning sferics associated with TGFs are measured at range as close as about 28 km with respect to equatorial thunderstorms
- Parent lightning of TGFs in the equatorial area bears the similar progressing features and height of thundercloud top to those at higher latitudes
- Nearly half TGFs are located in the strong but not the strongest convection region of varied-scale equatorial thunderstorms at the mature stage

Correspondence to:

G. Lu,
gaopenglu@gmail.com

Citation:

Zhang, H., Lu, G., Lyu, F., Ahmad, M. R., Qie, X., Cummer, S. A., et al. (2020). First measurements of low-frequency sferics associated with terrestrial gamma-ray flashes produced by equatorial thunderstorms. *Geophysical Research Letters*, 47, e2020GL089005. <https://doi.org/10.1029/2020GL089005>

Received 23 MAY 2020

Accepted 13 AUG 2020

Accepted article online 21 AUG 2020

First Measurements of Low-Frequency Sferics Associated With Terrestrial Gamma-Ray Flashes Produced by Equatorial Thunderstorms

Hongbo Zhang¹ , Gaopeng Lu^{2,3} , Fanchao Lyu⁴ , Mohd Riduan Ahmad⁵ , Xiushu Qie^{1,3} , Steven A. Cummer⁶ , Shaolin Xiong⁷ , and Michael S. Briggs⁸ 

¹Key Laboratory of Middle Atmosphere and Global Environment Observation (LAGEO), Institute of Atmospheric Physics, Chinese Academy of Sciences, Beijing, China, ²School of Earth and Space Sciences, University of Science and Technology of China, Hefei, China, ³Collaborative Innovation Center on Forecast and Evaluation of Meteorological Disasters, Nanjing University of Information Science and Technology, Nanjing, China, ⁴Department of Building Services Engineering, The Hong Kong Polytechnic University, Hong Kong, ⁵Atmospheric and Lightning Research Laboratory, Centre for Telecommunication Research and Innovation (CeTRI), Fakulti Kejuruteraan Elektronik dan Kejuruteraan Komputer, Universiti Teknikal Malaysia Melaka, Durian Tunggal, Malaysia, ⁶Electrical and Computer Engineering Department, Duke University, Durham, NC, USA, ⁷Key Laboratory of Particle Astrophysics, Institute of High Energy Physics, Chinese Academy of Sciences, Beijing, China, ⁸Center for Space Plasma and Aeronomics Research (CSPAR), University of Alabama in Huntsville, Huntsville, AL, USA

Abstract The low-frequency (LF) lightning sferics associated with terrestrial gamma-ray flashes (TGFs) detected by Fermi Gamma-ray Burst Monitor over equatorial thunderstorms have been recorded at a station in Melaka, Malaysia, since 2017. We examine the LF sferics of two Fermi TGFs, including one TGF-associated lightning discharge at only about 28 km range. Both TGFs are related to the strongest pulse during the initial stage of their parent intracloud (IC) lightning, while in both cases, the light curve of gamma-ray photon lags the major lightning pulse by approximately 100 μ s. TGF occurred about 3 ms after the lightning initiation when the initial upward negative leader has ascended for about 2 km to reach the height of 10–11 km. Our analyses on a statistical basis show that TGF-related lightning is mostly located in the strong convection of equatorial thunderstorms at the mature stage, and nearly half TGFs are not produced in the strongest convection region.

Plain Language Summary As one of the effects caused by tropospheric lightning in the near-Earth space, terrestrial gamma-ray flashes (TGFs) have been registered as worldwide phenomenon typically associated with deep convection of thunderstorms. Although the equatorial regions appear to be one of the hot spots for the spaceborne observations of TGFs, the ground-based measurements of TGF-associated lightning sferics have not been conducted so far near equator. Since the summer of 2017, a low-frequency (LF) magnetic field sensor has been installed on the campus of Universiti Teknikal Malaysia Melaka to record the radio frequency lightning signal associated with TGFs detected by Fermi. Due to the apparent proximity to the active region of TGF observations, the TGF-associated lightning signals have been recorded within 200 km for several cases during 2 year operation, including one recorded at a distance as close as 28 km. For another case with TGF-associated sferics recorded at 270 km range, the progression of negative upward leader can be tracked by examining the sequence of lightning pulses along with their ionospheric reflection. Through individual analysis and statistical research, the types, stages of TGF-related thunderstorms, and the positions of lightning source relative to storms are discussed in this paper.

1. Introduction

Terrestrial gamma-ray flashes (TGFs) are brief bursts of gamma-ray emissions with photon energies typically exceeding 1 MeV that are predominantly observed by spaceborne detectors on the low Earth orbit (Briggs et al., 2010; Marisaldi et al., 2010; Smith et al., 2005). The connection between TGFs and tropospheric thunderstorms was almost immediately established upon their discovery (Fishman et al., 1994). Lightning sferics measured at varying ranges are used to determine the relationship between TGFs and lightning (Cohen et al., 2010; Cummer et al., 2005, 2011; Stanley et al., 2006) and characterize electrical properties of TGF-related lightning discharges (Lu et al., 2011, 2019). More and more observations are reported to

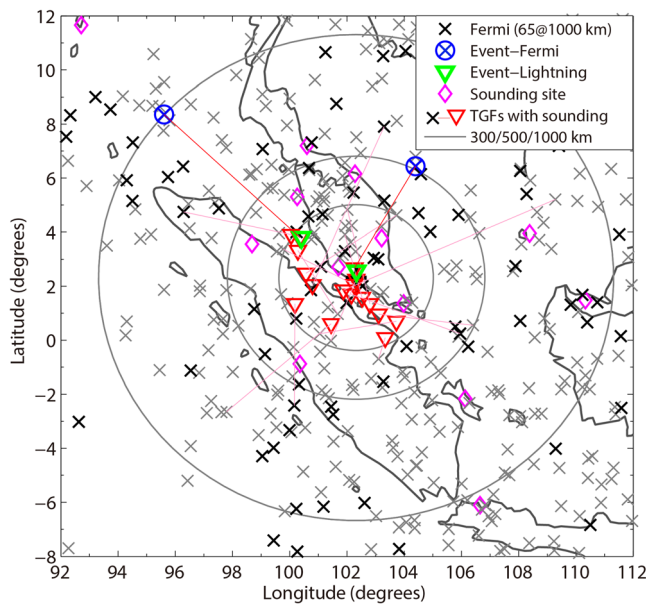


Figure 1. Schematic diagram of TGF observations in the geographic region centered at MALA station, detected by Fermi during May 2017 to December 2018 (black "x"s, while gray "x"s show all TGFs from 2008). The footprints of Events A and B and their related lightning locations given by GLD360 analyzed in section 3 are marked as blue "⊗"s and green "V"s. Pink "◊"s represent the weather radiosonde sounding sites, and red "▽"s represent the 17 TGF-related lightning locations given by GLD360, which were within 300 km of MALA station, and the sounding data near TGF time were available (connected with their footprints by pink lines).

TGFs and their parent lightning produced by tropical thunderstorms.

Nevertheless, TGFs produced by equatorial thunderstorms are most frequently observed by spaceborne detectors, and there is a much higher chance to acquire close observations and therefore more insight into the mechanism of TGF production with the measurement of broadband lightning signals in equatorial areas. In this paper, we summarize the measurement of radio frequency lightning sferics in 2017–2018 at a station located in Melaka, Malaysia, for TGFs detected by Fermi Gamma-ray Burst Monitor (GBM) (Briggs et al., 2010). In particular, we examine the sferics associated with two TGFs from lightning sources at the range of 28 and 270 km, respectively. The parent thunderstorms are also examined to reveal whether tropical thunderstorms bear favorable feathers for TGF production.

2. Measurements and Data

In order to characterize the lightning sferics associated with TGFs produced by equatorial thunderstorms, a broadband magnetic sensor composed of two orthogonal induction coils (e.g., Cummer et al., 2011) was installed on the campus of Universiti Teknikal Malaysia Melaka (UTeM) (referred to as MALA station hereinafter). Since the installation in May of 2017, the lightning signals in the frequency range of 10 to 400 kHz were continuously recorded at 1 MHz (with time accuracy better than 1 μ s) for TGFs detected by Fermi orbiting at \sim 560 km altitude with an inclination of 25.6° (Briggs et al., 2013). Figure 1 shows the Fermi footprint of TGFs around MALA station during May 2017 to December 2018, and there are totally 65 TGFs (black "x"s) detected over the footprint within 1,000 km of MALA station. (All Fermi TGFs detected prior to May of 2017 are shown as gray "x"s in Figure 1, demonstrating the occurrence of more TGFs near MALA station.)

Since the initial operation in summer of 2017, the low-frequency (LF) sferics with relatively high signal-to-noise ratio ($\text{SNR} \geq 10$) have been recorded for nearly 100 Fermi TGFs. Among the 65 events with Fermi footprint within 1,000 km range, the lightning discharge associated with 27 TGFs can be identified in the detection of either the World Wide Lightning Location Network (WWLLN) and/or Vaisala's Global Lightning

substantiate the connection between TGFs and the initial upward leader of ordinary bilevel intracloud (IC) lightning (Lu et al., 2010; Lyu et al., 2018; Østgaard et al., 2013; Shao et al., 2010). The TGF-associated lightning discharges are usually characterized by a relatively high peak current and the association with a moderate impulse charge transfer (Cummer et al., 2005; Lu et al., 2011, 2019; Lyu et al., 2015). Besides, downward TGFs were also observed on the ground in association with rocket-triggered lightning (Dwyer et al., 2004; Hare et al., 2016) and natural cloud-to-ground lightning (Abbasi et al., 2018; Tran et al., 2015; Wada et al., 2020).

The global distribution of TGFs detected from space resembles that of lightning by demonstrating three high distributions in Africa, Americas, and Southeast Asia, respectively (Grefenstette et al., 2009; Splitt et al., 2010). However, the examinations of TGF-associated lightning sferics predominantly regard events observed at middle latitudes (Cummer et al., 2011; Lu et al., 2010; Lyu et al., 2018), with limited studies on TGFs produced by tropical thunderstorms (e.g., Østgaard et al., 2013). Previous studies indicate that TGFs are usually related to the deep convection of parent thunderstorms (Smith et al., 2010; Splitt et al., 2010) with relatively high hydrometeor concentrations and convective available potential energy (CAPE) (Barnes et al., 2015; Fabrò et al., 2015), whose top typically reaches above 15 km (Chronis et al., 2016). As the tropopause is typically higher in the tropical areas (Fu, 2015), will the TGF-producing thunderstorms there develop a much higher top? If so, will the TGF-producing lightning bear some different features from that in subtropical areas? Some analyses showed that the tropopause altitude seems to be important but not primordial for TGF production (Smith et al., 2010), and there are no privileged thunderstorm conditions for TGF production (Chronis et al., 2016). Therefore, more efforts are desired to investigate

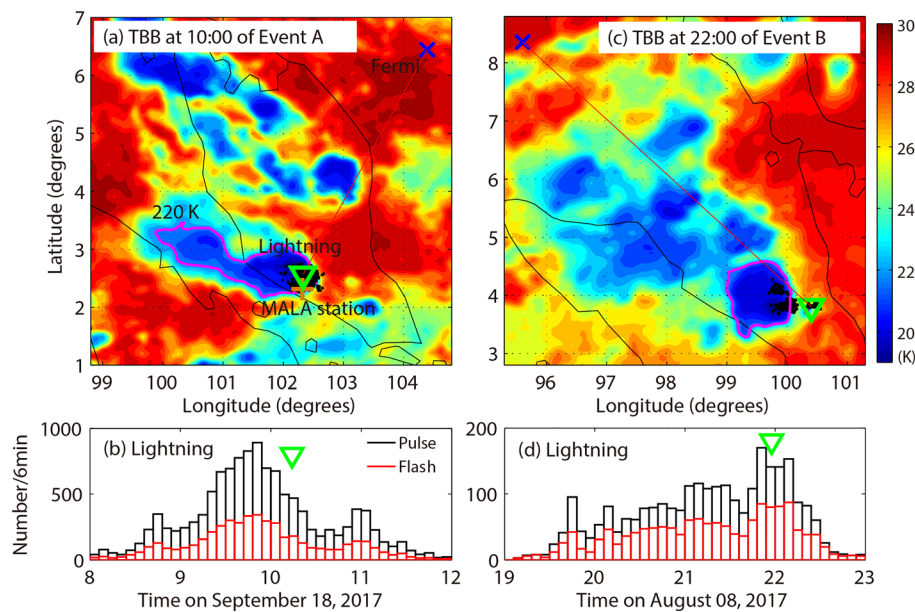


Figure 2. (a) Event A: TBB data at 10 UTC from Fengyun-2G satellite, overlapping with TGF source location (green "V") and 366 flashes (grouped from 977 lightning pulses location) between 1008 and 1020 UTC (black points). (b) Same as (a) but for Event B, TBB data at 22 UTC and 173 flashes (309 pulses) between 2152 and 2204 UTC. (c) Lightning frequency (over 6 min bin) during the parent thunderstorm on 18 September 2017. (d) Same as (c) but for the parent thunderstorm of Event B on 8 August 2017.

Dataset (GLD360). Here we apply the criteria of 5 ms offset after subtracting the propagation delay and 800 km distance between Fermi footprint and lightning location (e.g., Connaughton et al., 2010). Two events (referred to Event A and Event B, respectively, blue "⊗"s in Figure 1) are of our particular interest and are examined in section 3: The first case (Event A) was measured at a range of about 28 km from MALA station, which is the closest case ever reported for TGFs observed from space, although sferic measurements at even closer distances have been reported for downward TGFs observed on the ground surface (e.g., Tran et al., 2015); for the second case (Event B), the LF sferics measured at 270 km range exhibit multiple groups of ionosphere reflection, making it possible to investigate the progressing feature of TGF-producing lightning.

The black body temperature (TBB) data with temporal resolution of 1 hr and spatial resolution of 1 km captured by Chinese geostationary satellite Fengyun-2G are examined to characterize TGF-producing thunderstorms. We also refer to the weather sounding (<http://weather.uwyo.edu/upperair/sounding.html>) at several stations nearby to obtain the temperature profile and CAPE value.

3. Case Studies

The lightning discharge associated with two events (green "V"s in Figures 1 and 2) to be examined were both detected by GLD360 (which also gives the estimated peak current and polarity (positive means that negative charge is raised, or equivalently, positive charge is lowered)) and WWLLN. The TBB data upon the TGF observation show that both TGFs occurred at the mature stage of parent thunderstorm. As shown in Figure 2, the lightning discharge associated with Event A was located almost at the center of strong convection region, while that of Event B occurred at the edge of main strong convection.

3.1. Event A on 18 September 2017

Event A was detected by Fermi GBM at 1014:08.374 UTC on 18 September 2017 when the footprint was at (6.440°N, 104.396°E). The lightning discharge associated with this TGF was located by GLD360 at (2.567°N, 102.331°E), about 486 km from the Fermi footprint and only 28.2 km from MALA station, composing the closest sferic measurement ever reported for TGFs observed from space. The synchronous LF signal and photon data with time shifted back to the TGF source (similar processing with Pu et al., 2019) are shown

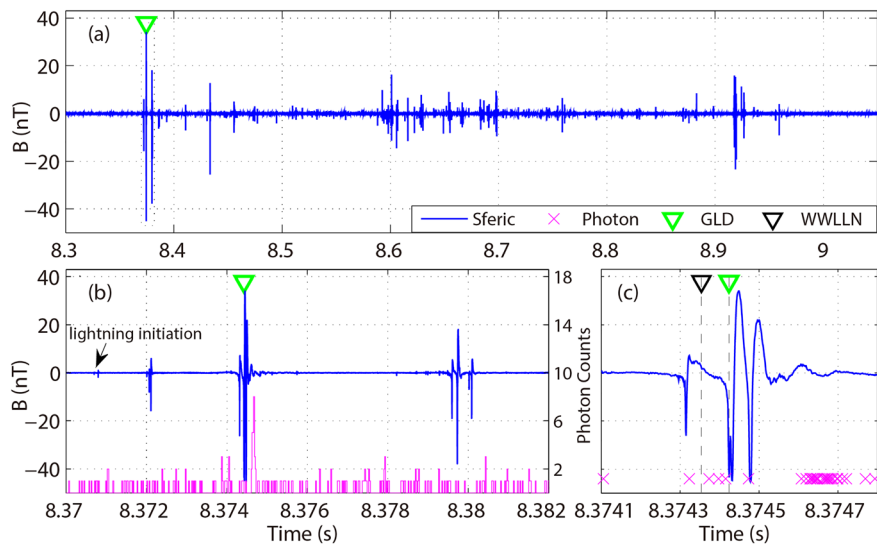


Figure 3. Time-corrected photon data and the TGF-related intracloud lightning sferic measured by MALA LF station (28.2 km away) in different time windows (a–c) of Event A. Blue line represents B field, and green “V” represents the occurrence time of lightning discharge given by GLD360, which is slightly different from that given by WWLLN (black “V,” caused by location error). Photon data recorded by Fermi and the histogram over 20 μ s bin are shown as pink “x”’s in (b) and (c).

in Figure 3. Owing to a close distance, the recorded LF signals contained a long sequence of pulses over 650 ms, strongly indicating the connection with IC lightning. The strongest pulse at 8.374423 s among all pulses of the IC is identified as the TGF-related lightning discharge (Figure 3b), whose peak current estimated by GLD360 is +35 kA, which is rather intense for IC discharges in this thunderstorm, while the TGF-associated pulse was not an energetic in-cloud pulse (EIP) (Lyu et al., 2015).

The photon data of Fermi shown in Figure 3c contain 25 photons over 114 μ s and peak at 8 counts (over 20 μ s bin), which lags the associated peak sferic about 250 μ s. With the location error of 1.8 km given by GLD360, by placing the TGF source at a height of 10–12 km (e.g., Lu et al., 2010; Shao et al., 2010), the maximum uncertainty in the temporal correlation between the light curve (i.e., the time-resolved variation of gamma-ray counts in certain bin) and TGF-related sferic pulse is estimated to be 4.1 μ s. That is, even taking the location uncertainty and the pulse duration into account, the time difference between the lightning pulse and gamma-ray curve is over 110 μ s; namely, the peak lightning sferic and TGF photon are not well synchronized in this particular case.

In addition to the major TGF-related signal, there are several other pulses before and after the TGF production. The first fast bipolar pulse barely discernible at about 3.6 ms prior to the gamma-ray production is attributed to the onset of initial breakdown (IB) stage of lightning flash. The IB stage lasted about 17 ms with six bursts of IBPs (Marshall et al., 2013). Following that, there are tens of weaker pulses reflecting the upward progression of initial negative leader. In general, the interpretation of sferic recorded at 28.2 km range for Event A is similar to the measurements examined by Shao et al. (2010) and Lu et al. (2019) for TGFs detected by the Reuven Ramaty High Energy Solar Spectroscopic Imager (RHESSI).

The TBB data from Fengyun-2G satellite at 10 UTC are shown in Figure 2a. The TBB value at the TGF source position was about 195 K, and almost at the center of the wide range “cold” region (the area of region lower than 220 K [pink line in Figure 2a] is about 18,000 km², and the minimum is 194.4 K), indicating the development of a strong convection. The TGF was almost produced in the strongest convection region (e.g., Chronis et al., 2016). Figure 2c shows the histogram (6 min bin) of lightning frequency during the parent thunderstorm of Event A. When the TGF was detected, the thunderstorm was at the mature stage, and the lightning rate was 180 flashes per 6 min.

Unfortunately, although the close distance makes it possible to see many details regarding the evolution of TGF-associated lightning, especially during its initial stage, it also caused the waveform substantial

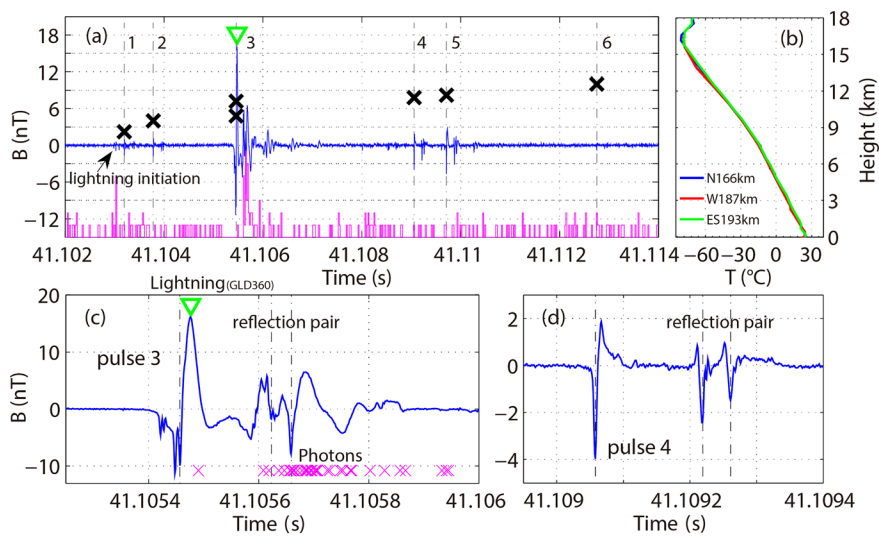


Figure 4. (a) Overview of time-corrected TGF-related IC lightning sferics (at 270 km) of Event B. Blue line represents B field, and the photon detection by Fermi is shown as pink "S"s. Six pulses (numbered as 1–6) with obvious ionosphere reflection are marked as gray dashed line. The height of individual pulses is marked with black "x." (b) Radiosonde sounding data at 00 UTC, 9 August, from three stations (Penan, 166 km north of the lightning location; Medan, 187 km west; and Sepang, 193 km southeast). (c) Eight hundred microseconds of LF data showing Pulse 3 associated with TGF. (d) Four hundred fifty microseconds of data showing Pulse 4, and its ionosphere reflection pair used to single station locate the pulse's height.

saturation. There is no clear ionospheric reflection that can be examined with the method described by Cummer et al. (2015) to infer the height of TGF source and other IC discharges that occur as a sequence.

3.2. Event B on 8 August 2017

Event B was recorded at 2157:41.109 UTC on 8 August 2017 when the footprint of Fermi GBM was at (8.355°N, 95.605°E). GLD360 located the TGF-associated lightning discharge at (3.805°N, 100.403°E), which is about 733 km from the Fermi footprint and 269.7 km from MALA station. WWLLN located the discharge at a similar location. As shown in Figure 4, the TGF light curve contains 29 photons over 160 μs and peaks at 7 counts (over 20 μs bin). At a relatively far distance, the lightning sferic shows a sequence of ≥10 discernible pulses over 10 ms, resembling IBPs examined by Marshall et al. (2013). The largest pulse inferred to be associated with TGF has a peak current of 92 kA (but GLD360 identified it as negative, probably due to overshoot in the recorded waveform), likely an EIP (Lyu et al., 2015). The TGF-related discharge occurred about 2.5 ms after the inferred lightning initiation.

For this event, the TGF-related signals contain clear ionospheric reflections that help to determine the height of individual lightning pulses and therefore infer the progressing feature of lightning leader (e.g., Cummer et al., 2015; Shao et al., 2010). The polarity of all these pulses indicates the radiation from the stepwise propagation of a negative upward leader (e.g., Cummer et al., 2015; Shao et al., 2010). As the source location of these pulses is given by GLD360, with the time lag between the ground wave and ionospheric reflection of each pulse, the equivalent reflection height is estimated to be 89.0 km (e.g., Zhang et al., 2016). Then, the height and distance from MALA station are calculated for each pulse. For Pulse 4 (Figure 4d), the time lag is 161 and 202 μs, respectively, and the height and distance are estimated (with the least squares method) to be 11.4 km (above the mean sea level [msl]) and 271.2 km, respectively. For Pulse 3 with relatively complicated waveform, the possible peaks of reflections were first identified with the roughly time lag (calculated with 2-D location and the heights between that of Pulses 2 and 4) to estimate the actual range of time lags, and then we constrain the height in the range of 9.9 to 11.1 km. The estimated height of Pulses 1–6 (indicated in Figure 4a) indicates the upward propagation of a negative leader from about 8.6 to 12.5 km (msl). The average speed for the vertical propagation of negative leader is thus estimated to be 3.7×10^5 m/s, generally consistent with previous analyses (ranging between 0.4×10^6 and 1.0×10^6 m/s) (e.g., Cummer et al., 2015; Shao et al., 2010). Note that for Event B, the zenith angle between TGF-related

lightning and Fermi satellite is estimated to be 54.2° , larger than the typical value ($\sim 30\text{--}40^\circ$, Gjesteland et al., 2011). The relatively large lateral offset might imply that the leader channel could be substantially tilted away from vertical (e.g., Lyu et al., 2016), although this could not be revealed with the inferred horizontal distance from MALA station due to the relatively large uncertainty in range estimation. In summary, Event B is associated with the strongest pulse of IC that appeared at 2.5 ms after the lightning initiation, when the negative leader has propagated upward for about 2 km.

The photon data lag the major TGF pulse about 220 μs . Similar to Event A, with the location error of 3.6 km given by GLD360 and the calculated height of major TGF pulse (Pulse 3), the maximum uncertainty in the temporal correlation between the light curve and TGF-related sferic is estimated to be 6.1 μs . Taking the location uncertainty and the pulse width into account, the photon data still correspond to the small signal about 100 μs after Pulse 3, and the peak lightning sferic and TGF photon are not simultaneous to each other.

The Fengyun-2G TBB data at 22 UTC are shown in Figure 2b, overlapping with 309 pulses and 173 flashes from 2152 to 2204 UTC. The "cold" region lower than 220 K was about 24.2 km^2 , and the minimum TBB was 218.5 K. The value of TGF source position is 234 K, 4 km away from the "cold" region. On the left side (25 km away), there is a large and colder region with size of "cold" region up to $12,500 \text{ km}^2$ and minimum TBB of 193.5 K, indicating that the thunderstorm developed much stronger than the TGF-related region. Most lightning strokes located in the left "cold" region, with only several lightning in the right "cold" region, which agrees with the TBB distribution. Besides, TGF occurred at the edge of right-side strong convection. Figure 2d shows the lightning frequency (with 6 min bin) during the parent thunderstorm of Event B. Upon the TGF observation, the thunderstorm was at the mature stage, and the lightning rate was 80 flashes per 6 min, almost highest during the thunderstorm.

4. Discussions and Conclusions

The analyses of two Fermi TGFs in section 3 are generally consistent with the scenario that the gamma rays are produced by the initial upward negative leader of normal bilevel IC lightning (e.g., Lu et al., 2010; Østgaard et al., 2013). The parent lightning of Event A lasted about 650 ms with abundant IC discharges identified from the sferic measurement due to its close distance (28.2 km) from MALA station. For Event B, the single-station location results show that the TGF occurred at about 10–11 km when the negative leader has propagated upward about 2 km. In two cases, the gamma-ray production occurred at 3.6 and 2.5 ms, respectively, after the lightning initiation, but the photon data of both events lag the major lightning pulse by about 100 μs . The time lag was conformed to be an observation fact rather than caused by data error after the analysis of other TGF data. The possible reason was inferred from the proposed TGF mechanisms: relativistic feedback model (e.g., Dwyer, 2012) and the lightning leader model (e.g., Celestin & Pasko, 2011). As the strongest pulse of the parent IC (significantly bigger than the previous pulse), the TGF-associated leader discharge may produce a certain number of electrons/photons (as seeds of coming TGF), instead of producing enough upward photons to form a Fermi-observed TGF. Then, during the time lag about 100 μs , more electrons/photons are further produced through relativistic runaway electron avalanches to form the observed TGF under the strong electric field at the tip of leader; they could also be generated under the ambient electric field near lightning. More data and model simulation are needed to explain this phenomenon in the future.

The thunderstorm generally develops a higher cloud top at lower latitude; namely, the height of equatorial thunderstorm is typically higher than other regions (Fu, 2015). However, as analyzed in section 3.2, the source height of Event B is located at 9.9–11.1 km, which is similar to the results at middle latitudes (Cummer et al., 2014; Pu et al., 2019; Shao et al., 2010). Meteorological sounding data could provide the developing height of thunderstorms and typical temperature layers, which is closely connected to the charge layers in thundercloud. As shown in Figure 5a, the sounding results of 17 TGFs within 300 km of MALA station are quite similar, and the red points representing the heights of four temperature layers (0°C , -10°C , -20°C , and -30°C) are at similar height (varies within 1 km). In contrast, the sounding data of 17 TGFs occurred in south China (with latitude ranging from 20.2°N to 25.7°N) are shown in Figure 5b. The profiles in equatorial regions and southern China exhibit almost same features; even those at higher latitudes are slightly higher (about 600 m), which may be caused by the larger CAPE as shown in Figures 5a and 5b.

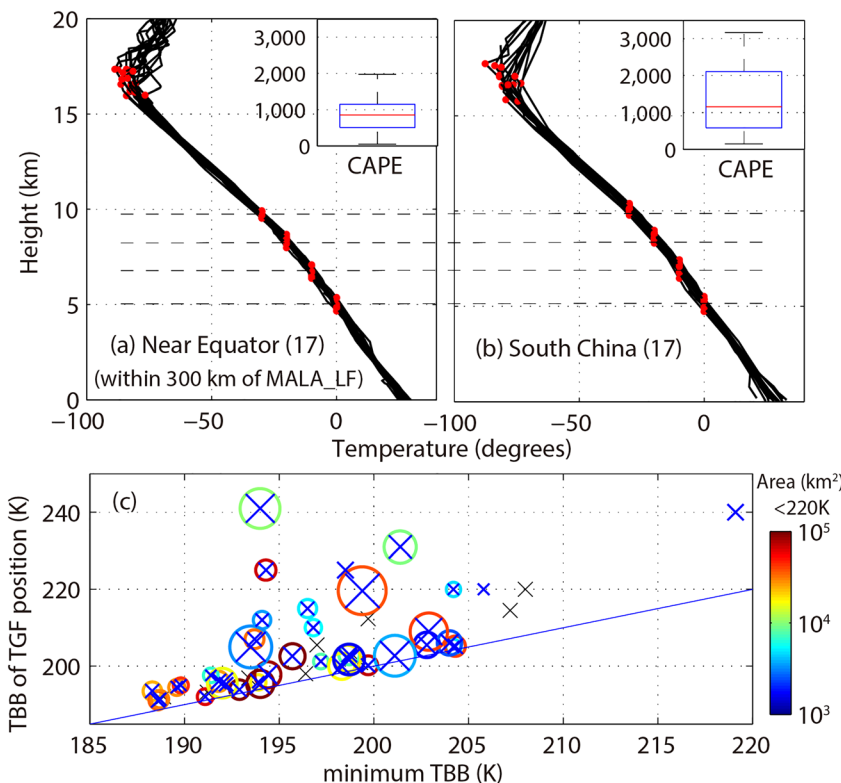


Figure 5. (a) Temperature profiles from the radiosonde sounding for 17 equatorial Fermi TGFs (red "V"s in Figure 1). Heights of four-temperature layer (0°C , -10°C , -20°C , and -30°C) of each profile are marked as red points. The inset is the CAPE box plot of 17 TGF cases. (b) Similar to (a) but for 17 TGFs related to lightning discharges in south China (with latitude between 20.2°N and 25.7°N), showing similar temperature profiles to equatorial regions. (c) Comparison between the TBB value at the source location of 50 TGFs and the minimum value of TGF-producing thunderstorms. The circle size represents the peak current of TGF-related lightning, and the color means the area of thunderstorms where $\text{TBB} < 220 \text{ K}$.

Therefore, the heights of TGF production in equatorial thunderstorms appear not to be considerably different from the cases in south China.

The parent thunderstorms of two TGFs are similar in several aspects. Both occurred at the mature stage of parent thunderstorm. For Event A, it was located almost at the center of strong convection, while Event B was produced at the edge of strong convection. The analyses of TBB data for 50 TGFs produced by equatorial thunderstorms (94°E to 110°E , -4°N to 8°N) indicate that the size of these storms varies over a wide range from 1,500 to 280,000 km 2 (defined with the 220 K contour line, Figure 5c), which is consisted with Split et al. (2010), and the TGFs mostly occurred at the mature stage of thunderstorms (Ursi et al., 2019). The peak current of these TGFs reported by GLD360 also ranges widely from +27 to +507 kA. In comparison with normal IC discharges, the TGF-associated discharges often carry higher peak current (e.g., Lu et al., 2011, 2019). Figure 5c shows the TBB data at the TGF source location and the TBB minimum of parent thunderstorms for 50 TGFs. The TBB minimum ranges from 188.3 to 219.1 K, with average 197.3 K, while TBB source position ranges from 191.0–253.0 K with average 206.5 K. Therefore, almost all TGFs (48/50) are located in the relatively "cold" region of parent thunderstorms, with 25 events (52%) near the center of "cold" region and 23 (48%) at the edge. We also analyzed 13 TGFs detected over the mainland of China with TBB and weather radar data available, finding that seven TGFs (54%) occurred at the edge of "cold" region from the TBB data, while 11 TGFs (85%) were at the edge of convection (radar data are more reliable). The difference of center/edge ratio between TBB and radar data may be due to the relatively low spatial/temporal resolution of TBB data and incomplete correspondence between TBB and radar. However, the results at least suggest that TGFs are not always produced at the center of "cold" region, and nearly half TGFs occur in the strong, but not the strongest convection region of parent thunderstorms.

We also examine the LF signals of lightning discharges within 5 min in the vicinity of two TGF-associated discharges that were in the detection range (about 800 km) of Fermi GBM. There is no additional lightning discharge found corresponding to photon pulse, even some IC discharges with higher current (including one IC with similar characteristics to Event A). Therefore, it is still unclear why some lightning could produce TGFs, which might be answered by closer TGFs with comprehensive measurements. In the future, the TGF detections by Fermi, Atmosphere-Space Interaction Monitor (ASIM) (Neubert et al., 2019), and Chinese Hard X-ray Modulation Telescope (*Insight-HXMT*) (Zhang et al., 2020) will be examined with coordinated measurements to obtain a comprehensive understanding on the TGF production in equatorial thunderstorms.

Data Availability Statement

The data used for this analysis are available on the data repository website (<https://zenodo.org/record/3977245#.XzDj7FwzaUk>).

Acknowledgments

The research was supported by the National Key R&D Program of China (2017YFC1501501) and the National Natural Science Foundation of China (41622501, 41805004, 41875006, and U1938115). We thank the Fermi team for the TGF data (<https://heasarc.gsfc.nasa.gov/FTP/fermi/data/gbm/daily/>) and Vaisala for providing the GLD360 data used in this paper (<https://www.vaisala.com/en/products/data-subscriptions-and-reports/data-sets/gld360>). The authors also wish to thank the World Wide Lightning Location Network (<http://wwlln.net>) as a collaboration among over 50 universities and institutions, and Earth Networks Total Lightning Network (<https://www.earthnetworks.com/product/lightning-data/>) for providing the lightning data. Yunjiao Pu provided help on identifying the Fermi TGFs for further analyses. The Fengyun-2G satellite images are provided by the National Satellite Meteorological Center (NSMC) of China. Thanks to two anonymous reviewers for their valuable suggestions.

References

- Abbasi, R. U., Abu-Zayyad, T., Allen, M., Barcikowski, E., Belz, J. W., Bergman, D. R., et al. (2018). Gamma ray showers observed at ground level in coincidence with downward lightning leaders. *Journal of Geophysical Research: Atmospheres*, 123, 6864–6879. <https://doi.org/10.1029/2017JD027931>
- Barnes, D. E., Splitt, M. E., Dwyer, J. R., Lazarus, S., Smith, D. M., & Rassoul, H. K. (2015). A study of thunderstorm microphysical properties and lightning flash counts associated with terrestrial gamma-ray flashes. *Journal of Geophysical Research: Atmospheres*, 120, 3453–3464. <https://doi.org/10.1002/2014JD021495>
- Briggs, M. S., Fishman, G. J., Connaughton, V., Bhat, P. N., Paciesas, W. S., Preece, R. D., et al. (2010). First results on terrestrial gamma ray flashes from the Fermi Gamma-ray Burst Monitor. *Journal of Geophysical Research*, 115, A07323. <https://doi.org/10.1029/2009JA015242>
- Briggs, M. S., Xiong, S., Connaughton, V., Tierney, D., Fitzpatrick, G., Foley, S., et al. (2013). Terrestrial gamma-ray flashes in the Fermi era: Improved observations and analysis methods. *Journal of Geophysical Research: Space Physics*, 118, 3805–3830. <https://doi.org/10.1002/jgra.50205>
- Celestin, S., & Pasko, V. P. (2011). Energy and fluxes of thermal runaway electrons produced by exponential growth of streamers during the stepping of lightning leaders and in transient luminous events. *Journal of Geophysical Research*, 116, A03315. <https://doi.org/10.1029/2010JA016260>
- Chronis, T., Briggs, M. S., Priftis, G., Connaughton, V., Brundell, J., Holzworth, R., et al. (2016). Characteristics of thunderstorms that produce terrestrial gamma ray flashes. *Bulletin of the American Meteorological Society*, 97(4), 639–653. <https://doi.org/10.1175/BAMS-D-14-00239.1>
- Cohen, M. B., Inan, U. S., Said, R. K., & Gjesteland, T. (2010). Geolocation of terrestrial gamma-ray flash source lightning. *Geophysical Research Letters*, 37, L02801. <https://doi.org/10.1029/2009GL041753>
- Connaughton, V., Briggs, M. S., Holzworth, R. H., Hutchins, M. L., Fishman, G. J., Wilson-Hodge, C. A., et al. (2010). Associations between Fermi Gamma-ray Burst Monitor terrestrial gamma ray flashes and sferics from the World Wide Lightning Location Network. *Journal of Geophysical Research*, 115, A12307. <https://doi.org/10.1029/2010JA015681>
- Cummer, S. A., Briggs, M. S., Dwyer, J. R., Xiong, S., Connaughton, V., Fishman, G. J., et al. (2014). The source altitude, electric current, and intrinsic brightness of terrestrial gamma ray flashes. *Geophysical Research Letters*, 41, 8586–8593. <https://doi.org/10.1002/2014GL062196>
- Cummer, S. A., Lu, G., Briggs, M. S., Connaughton, V., Xiong, S., Fishman, G. J., & Dwyer, J. R. (2011). The lightning-TGF relationship on microsecond timescales. *Geophysical Research Letters*, 38, L14810. <https://doi.org/10.1029/2011GL048099>
- Cummer, S. A., Lyu, F., Briggs, M. S., Fitzpatrick, G., Roberts, O. J., & Dwyer, J. R. (2015). Lightning leader altitude progression in terrestrial gamma-ray flashes. *Geophysical Research Letters*, 42, 7792–7798. <https://doi.org/10.1002/2015GL065228>
- Cummer, S. A., Zhai, Y., Hu, W., Smith, D. M., Lopez, L. I., & Stanley, M. A. (2005). Measurements and implications of the relationship between lightning and terrestrial gamma ray flashes. *Geophysical Research Letters*, 32, L08811. <https://doi.org/10.1029/2005GL022778>
- Dwyer, J. R. (2012). The relativistic feedback discharge model of terrestrial gamma ray flashes. *Journal of Geophysical Research*, 117, A02308. <https://doi.org/10.1029/2011JA017160>
- Dwyer, J. R., Rassoul, H. K., Al-Dayeh, M., Caraway, L., Wright, B., Chrest, A., et al. (2004). A ground level gamma-ray burst observed in association with rocket-triggered lightning. *Geophysical Research Letters*, 31, L05119. <https://doi.org/10.1029/2003GL018771>
- Fabró, F., Montanyà, J., Marisaldi, M., van der Velde, O. A., & Fuschino, F. (2015). Analysis of global terrestrial gamma ray flashes distribution and special focus on AGILE detections over South America. *Journal of Atmospheric and Solar-Terrestrial Physics*, 124, 10–20. <https://doi.org/10.1016/j.jastp.2015.01.009>
- Fishman, G. J., Bhat, P., Mallozzi, R., Horack, J., Koshut, T., Kouveliotou, C., et al. (1994). Discovery of intense gamma-ray flashes of atmospheric origin. *Science*, 264(5163), 1313–1316. <https://doi.org/10.1126/science.264.5163.1313>
- Fu, R. (2015). Global warming-accelerated drying in the tropics. *Proceedings of the National Academy of Sciences of the United States of America*, 112(12), 3593–3594. <https://doi.org/10.1073/pnas.1503231112>
- Gjesteland, T., Østgaard, N., Collier, A. B., Carlson, B. E., Cohen, M. B., & Lehtinen, N. G. (2011). Confining the angular distribution of terrestrial gamma ray flash emission. *Journal of Geophysical Research*, 116, A11313. <https://doi.org/10.1029/2011JA016716>
- Grefenstette, B. W., Smith, D. M., Hazelton, B. J., & Lopez, L. I. (2009). First RHESSI terrestrial gamma ray flash catalog. *Journal of Geophysical Research*, 114, A02314. <https://doi.org/10.1029/2008JA013721>
- Hare, B. M., Uman, M. A., Dwyer, J. R., Jordan, D. M., Biggerstaff, M. I., Caicedo, J. A., et al. (2016). Ground-level observation of a terrestrial gamma ray flash initiated by a triggered lightning. *Journal of Geophysical Research: Atmospheres*, 121, 6511–6533. <https://doi.org/10.1002/2015JD024426>

- Lu, G., Blakeslee, R. J., Li, J., Smith, D. M., Shao, X., McCaul, E. W., et al. (2010). Lightning mapping observation of a terrestrial gamma-ray flash. *Geophysical Research Letters*, 37, L11806. <https://doi.org/10.1029/2010GL043494>
- Lu, G., Cummer, S. A., Li, J., Han, F., Smith, D. M., & Grefenstette, B. W. (2011). Characteristics of broadband lightning emissions associated with terrestrial gamma ray flashes. *Journal of Geophysical Research*, 116, A03316. <https://doi.org/10.1029/2010JA016141>
- Lu, G., Zhang, H., Cummer, S. A., Wang, Y., Lyu, F., Briggs, M., et al. (2019). A comparative study on the lightning sferics associated with terrestrial gamma-ray flashes observed in Americas and Asia. *Journal of Atmospheric and Solar-Terrestrial Physics*, 183, 67–75. <https://doi.org/10.1016/j.jastp.2019.01.001>
- Lyu, F., Cummer, S. A., Krehbiel, P. R., Rison, W., Briggs, M. S., Cramer, E., et al. (2018). Very high frequency radio emissions associated with the production of terrestrial gamma-ray flashes. *Geophysical Research Letters*, 45, 2097–2105. <https://doi.org/10.1002/2018GL077102>
- Lyu, F., Cummer, S. A., Lu, G., Zhou, X., & Weinert, J. (2016). Imaging lightning intracloud initial stepped leaders by low-frequency interferometric lightning mapping array. *Geophysical Research Letters*, 43, 5516–5523. <https://doi.org/10.1002/2016GL069267>
- Lyu, F., Cummer, S. A., & McTague, L. (2015). Insights into high peak current in-cloud lightning events during thunderstorms. *Geophysical Research Letters*, 42, 6836–6843. <https://doi.org/10.1002/2015GL065047>
- Marisaldi, M., Fuschino, F., Labanti, C., Galli, M., Longo, F., Del Monte, E., et al. (2010). Detection of terrestrial gamma ray flashes up to 40 MeV by the AGILE satellite. *Journal of Geophysical Research*, 115, A00E13. <https://doi.org/10.1029/2009JA014502>
- Marshall, T., Stolzenburg, M., Karunarathne, S., Cummer, S. A., Lu, G., Betz, H. D., et al. (2013). Initial breakdown pulses in intracloud lightning flashes and their relation to terrestrial gamma ray flashes. *Journal of Geophysical Research: Atmospheres*, 118, 10,907–10,925. <https://doi.org/10.1002/jgrd.50866>
- Neubert, T., Østgaard, N., Reglero, V., Chanrion, O., Heumesser, M., Dimitriadou, K., et al. (2019). A terrestrial gamma-ray flash and ionospheric ultraviolet emissions powered by lightning. *Science*, eaax3872. <https://doi.org/10.1126/science.aax3872>
- Østgaard, N., Gjesteland, T., Carlson, B. E., Collier, A. B., Cummer, S. A., Lu, G., & Christian, H. J. (2013). Simultaneous observations of optical lightning and terrestrial gamma ray flash from space. *Geophysical Research Letters*, 40, 2423–2426. <https://doi.org/10.1002/grl.50466>
- Pu, Y., Cummer, S. A., Lyu, F., Briggs, M., Mailyan, B., Stanbro, M., & Roberts, O. (2019). Low frequency radio pulses produced by terrestrial gamma-ray flashes. *Geophysical Research Letters*, 46, 6990–6997. <https://doi.org/10.1029/2019GL082743>
- Shao, X. M., Hamlin, T., & Smith, D. M. (2010). A closer examination of terrestrial gamma-ray flash-related lightning processes. *Journal of Geophysical Research*, 115, A00E30. <https://doi.org/10.1029/2009JA014835>
- Smith, D. M., Hazelton, B. J., Grefenstette, B. W., Dwyer, J. R., Holzworth, R. H., & Lay, E. H. (2010). Terrestrial gamma ray flashes correlated to storm phase and tropopause height. *Journal of Geophysical Research*, 115, A00E49. <https://doi.org/10.1029/2009JA014853>
- Smith, D. M., Lopez, L. I., Lin, R. P., & Barrington-Leigh, C. P. (2005). Terrestrial gamma-ray flashes observed up to 20 MeV. *Science*, 307(5712), 1085–1088. <https://doi.org/10.1126/science.1107466>
- Splitt, M. E., Lazarus, S. M., Barnes, D., Dwyer, J. R., Rassoul, H. K., Smith, D. M., et al. (2010). Thunderstorm characteristics associated with RHESSI identified terrestrial gamma ray flashes. *Journal of Geophysical Research*, 115, A00E38. <https://doi.org/10.1029/2009JA014622>
- Stanley, M. A., Shao, X. M., Smith, D. M., Lopez, L. I., Pongratz, M. B., Harlin, J. D., et al. (2006). A link between terrestrial gamma-ray flashes and intracloud lightning discharges. *Geophysical Research Letters*, 33, L06803. <https://doi.org/10.1029/2005GL025537>
- Tran, M. D., Rakov, V. A., Mallick, S., Dwyer, J. R., & Heckman, S. (2015). A terrestrial gamma-ray flash recorded at the lightning observatory in Gainesville, Florida. *Journal of Atmospheric and Solar-Terrestrial Physics*, 136, 86–93. <https://doi.org/10.1016/j.jastp.2015.10.010>
- Ursi, A., Marisaldi, M., Dietrich, S., Tavani, M., Tiberia, A., & Porcu, F. (2019). Analysis of thunderstorms producing Terrestrial Gamma ray Flashes with the Meteosat Second Generation. *Journal of Geophysical Research: Atmospheres*, 124, 12,667–12,682. <https://doi.org/10.1029/2018JD030149>
- Wada, Y., Enoto, T., Nakamura, Y., Morimoto, T., Sato, M., Ushio, T., et al. (2020). High peak-current lightning discharges associated with downward terrestrial gamma-ray flashes. *Journal of Geophysical Research: Atmospheres*, 125, e2019JD031730. <https://doi.org/10.1029/2019JD031730>
- Zhang, H., Lu, G., Qie, X., Jiang, R., Fan, Y., Tian, Y., et al. (2016). Locating narrow bipolar events with single-station measurement of low-frequency magnetic fields. *Journal of Atmospheric and Solar-Terrestrial Physics*, 143–144, 88–101. <https://doi.org/10.1016/j.jastp.2016.03.009>
- Zhang, S., Li, T., Lu, F., Song, L., Xu, Y., Liu, C., et al. (2020). Overview to the Hard X-ray Modulation Telescope (Insight-HXMT) satellite. *Science China Physics, Mechanics & Astronomy*, 63, 249502. <https://doi.org/10.1007/s11433-019-1432-6>